An Overview of Tilting Pad Journal Bearings

Dr. Luis San Andres
Dept. of Mechanical Engineering
Texas A&M University
College Station, TX 77843-3123
Off: (979) 845-0160; Fax (979) 845-3081
E-Mail: LsanAndres@mengr.tamu.edu

February 2nd, 2000

These notes are based on original notes prepared by Dr. Ravindra Gadangi, Turbocare, Inc., Houston, 1995. The original also uses information from Univ. of Virginia, Class Notes for ME543.

AN OVERVIEW OF TILTING PAD JOURNAL BEARINGS

Rotating machines like compressors, turbines, pumps, electric motors, and electric generators are commonly supported in fluid film bearings. In the recent past, the bearings supports incorporated plain cylindrical bearings of simple design. The need to increase the efficiency and power output of typical turbomachines has brought them to operate at higher speeds with tighter clearances. These operations, however, are also accompanied with rotor-bearing hydrodynamic instabilities, i.e. high amplitude subsynchronous vibrations due to oil whirl or whip. Other types of bearing geometries have been devised to reduce the potential of subsynchronous whirl. Some of these bearings include axial grooves to provide a different oil flow pattern across the lubricated surface, while others have various patterns of variable clearance creating a converging film thickness even for the centered journal position. These are named preloaded multiple pad bearings since they are able to generate a direct stiffness at the journal concentric operation, thus increasing the rotor-bearing critical speeds and delaying the onset of whirl. Tilting pad bearings, however, offer an unsurpassed advantage, since each pad is able to rotate about a pivot thus attaining its own equilibrium position, with a strongly converging film region for each loaded pad. Tilting pad bearings have no cross-coupled stiffnesses for certain load conditions, and offer an operation free of subsynchronous whirl.

TYPES OF HYDRODYNAMIC BEARINGS:

(1) **Fixed Geometry Bearings**:

360° Plain journal bearing, partial arc journal bearing, pressure dam and lobed bearings. Sketches of these bearings are shown in Figures 1 and 2.

(2) **Tilting Pad Bearings**:

The bearing pads are free to move about a pivot, line or point. The number of pads, preload, pivot offset, and load direction can be varied to achieve the desired performance. A sketch of a tilting pad journal bearing is shown in Figure 3.

Table 1 summarizes the advantages and disadvantages of various radial bearings.

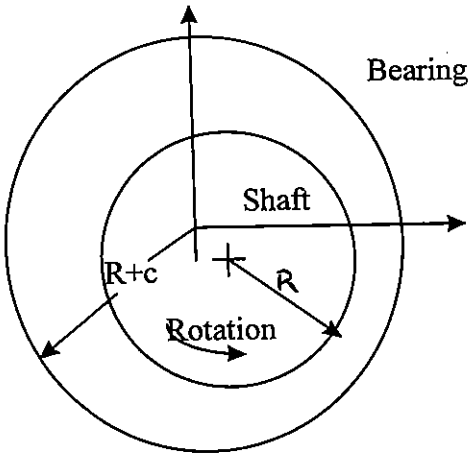

(a) Plain Journal Bearing

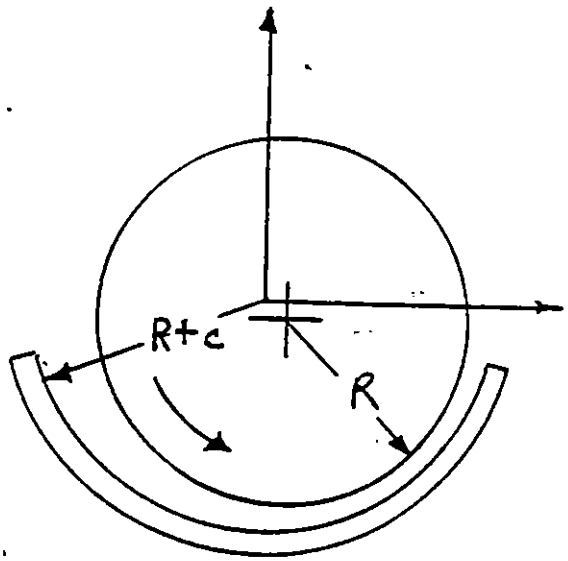

(b) 150° Partial Arc Bearing

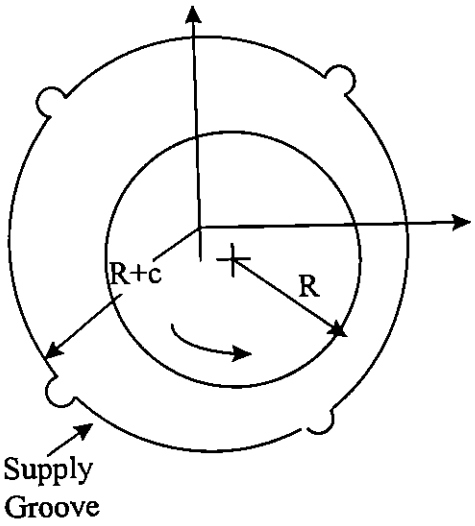

(c) Four Axial Groove Bearing

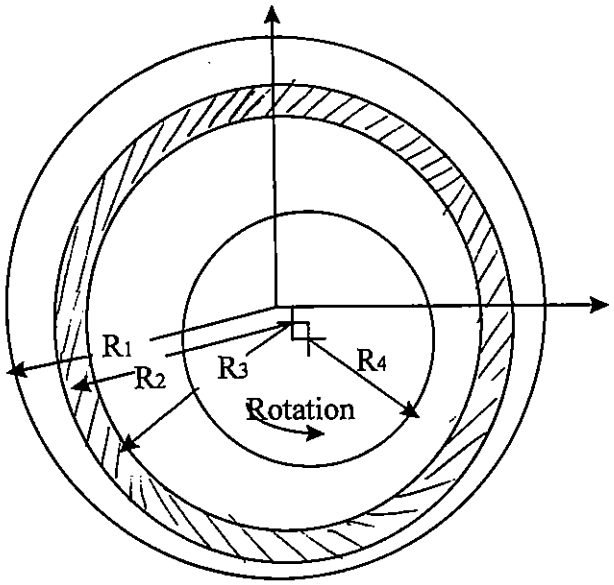

(d) Floating Ring Bearing

Figure 1. Types of fixed pad journal bearings without preload.

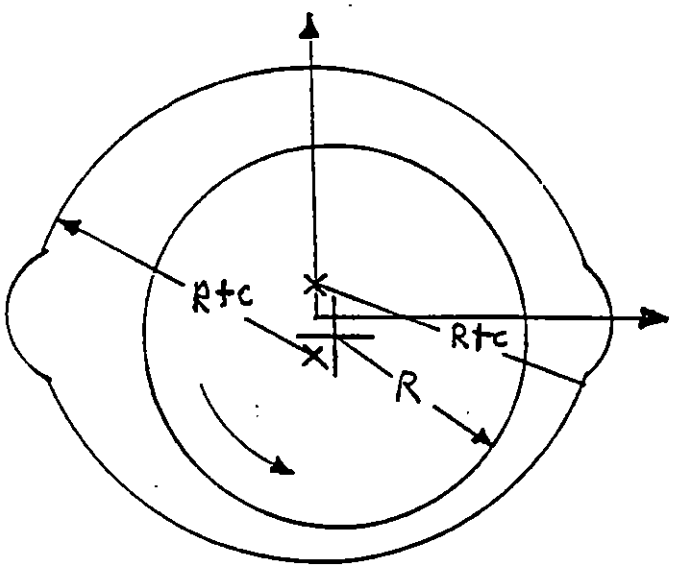

(a) Elliptical or Lemon Bore Bearing ($\alpha = 0.50$, $m = 0.4$)

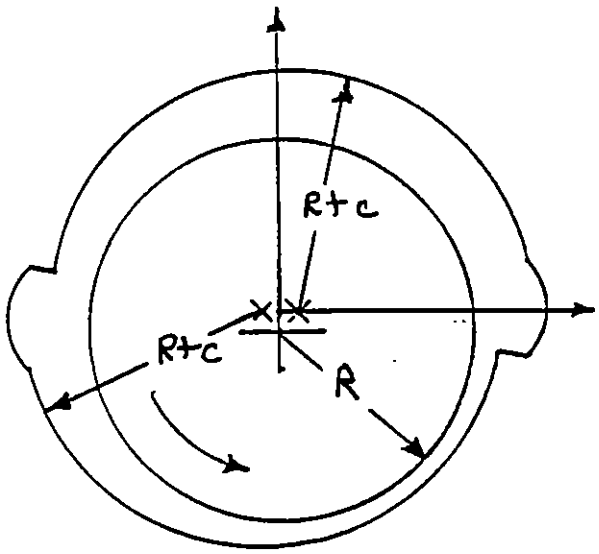

(b) Offset Half Bearing ($\alpha = 1.125$, $m = 0.4$)

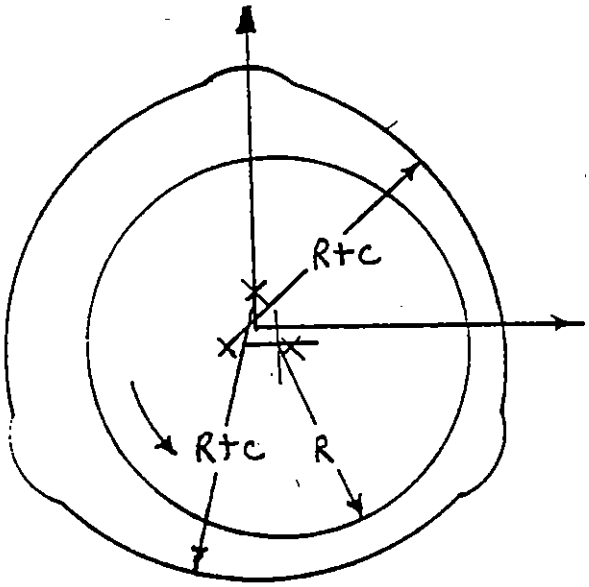

(c) Three Lobe Bearing ($\alpha = 0.50$, $m = 0.4$)

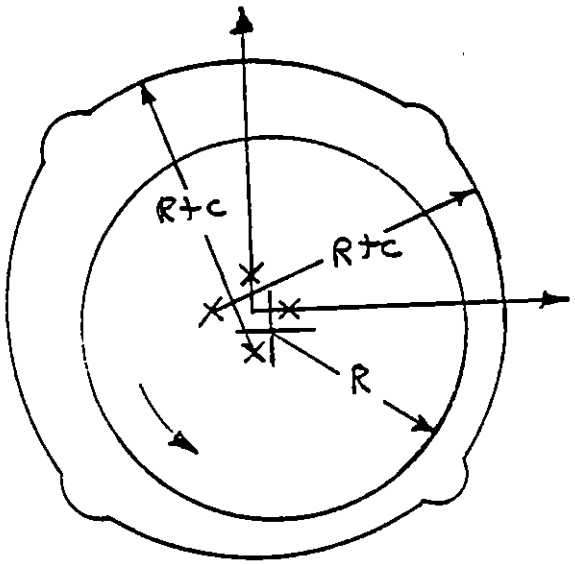

d) Four Lobe Bearing ($\alpha = 0.50$, $m = 0.40$)

Figure 2. Types of fixed pad journal bearings with preload.

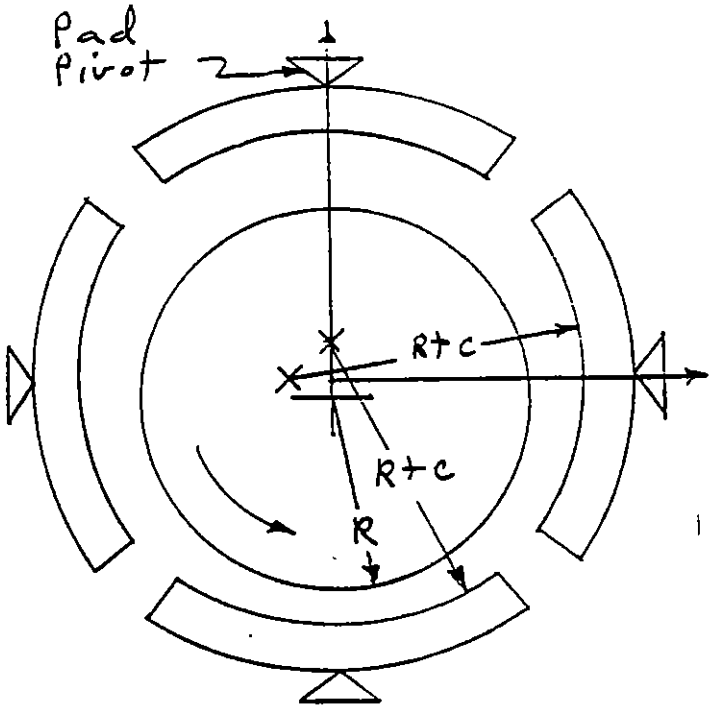

(a) Four Pad (Shoe) Tilting Pad

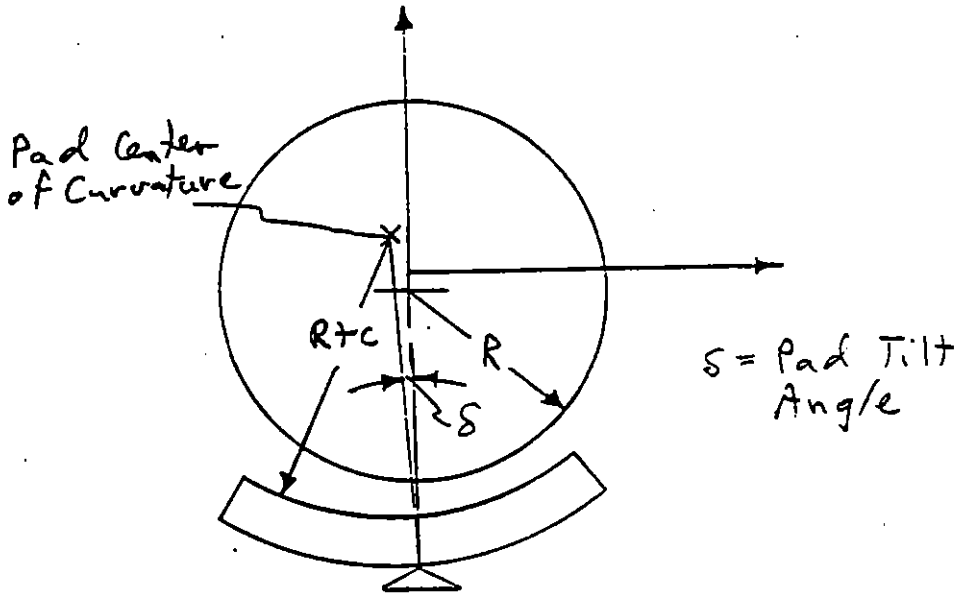

(b) Bottom pad shown in tilted position with converging film thickness

Figure 3. Tilting Pad Bearing Geometry

TABLE 1. FIXED PAD NON-PRE-LOADED JOURNAL BEARINGS

Bearing Type	Advantages	Disadvantages	Comments
Plain Journal	1. Easy to make 2. Low Cost	1. Very subject to oil whirl	Round bearings are nearly always "crushed" to make elliptical bearings
Partial Arc	1. Easy to make 2. Low Cost 3. Low horsepower loss	1. Poor vibration resistance 2. Oil supply not easily contained	Bearing used only on rather old machines
Axial Groove	1. Easy to make 2. Low Cost	1. Subject to oil whirl	Round bearings are nearly always "crushed" to make elliptical or multi-lobe
Floating Bush	1. Relatively easy to make 2. Low Cost	2. Subject to oil whirl	Used primarily in high speed turbochargers for diesel engines in trucks and buses
Elliptical	1. Easy to make 2. Low Cost 3. Good damping at critical speeds	1. Subject to oil whirl at high speeds 2. Load direction must be known	Probably most widely used bearing at low or moderate speeds
Offset Half (With Horizontal Split)	1. Excellent suppression of whirl at high speeds 2. Low Cost 3. Easy to make	1. Fair suppression of whirl at moderate speeds 2. Load direction must be known	Has high horizontal stiffness and low vertical stiffness - may become popular - used outside U.S.
Three and Four Lobe	1. Good suppression of whirl 2. Overall good performance 3. Moderate cost	1. Some types can be expensive to make properly 2. Subject to whirl at high speeds	Currently used by some manufacturers as standard bearing design

TABLE 1. FIXED PAD JOURNAL BEARINGS WITH STEPS, DAMS OR POCKETS

Bearing Type	Advantages	Disadvantages	Comments
Pressure Dam (Single Dam)	1. Good suppression of whirl 2. Low cost 3. Good damping at critical speeds 4. Easy to make	1. Goes unstable with little warning 2. Dam may be subject to wear or build up over time 3. Load direction must be known	Very popular with petro-chemical industry; Easy to convert elliptical over to pressure dam
Multi-Dam Axial Groove or Multi-Lobe	1. Dams are relatively easy to place in existing bearings 2. Good suppression of whirl 3. Relatively low cost 4. Good overall performance	1. Complex bearing requiring detailed analysis 2. May not suppress whirl due to nonbearing causes	Used as standard design by some manufacturers
Hydrostatic	1. Good suppression of oil whirl 2. Wide range of design parameters 3. Moderate cost	1. Poor damping at critical speeds 2. Requires careful design 3. Requires high pressure lubricant supply	Generally high stiffness properties used for high precision rotors

NON-FIXED PAD JOURNAL BEARING

Bearing Type	Advantages	Disadvantages	Comments
Tilting Pad	1. Will not cause whirl (no cross coupling) for certain load configurations.	1. High Cost 2. Requires careful design 3. Poor damping at critical speeds 4. Hard to determine actual clearances 5. High horsepower loss	Widely used bearing to stabilize machines with subsynchronous non-bearing excitations

TILTING PAD JOURNAL BEARINGS

Tilting pad (or Mitchell) bearings have been known since last century. This bearing has a geometry similar to a multiple-lobe bearing or an axial-groove bearing except that each individual shoe or pad is free to rock on an axial line-pivot or rock and pitch on a point pivot. This enables each pad on the bearing to follow the motion of the shaft, thereby decreasing the destabilizing cross-coupling forces usually seen in other types of fixed lobed bearings.

It has been known for many years that fluid film bearings such as the plain journal bearing contribute destabilizing cross-coupling forces to rotor-bearing systems. This bearing-induced instability is often called oil whirl. Because of this instability, machines operating in fixed lobed bearings are often limited in speed to around a maximum of 6,000 rpm. The tilting pad bearing, however, has virtually eliminated oil whirl instability and increased the maximum operating speed of rotor-bearing systems from 6,000 to 10,000 or even 14,000 rpm.

In fixed geometry bearings the hydrodynamic pressure profile generated is such that for a load applied in one direction, the shaft is pushed in an orthogonal direction. Figure 4 shows a sketch of this condition.

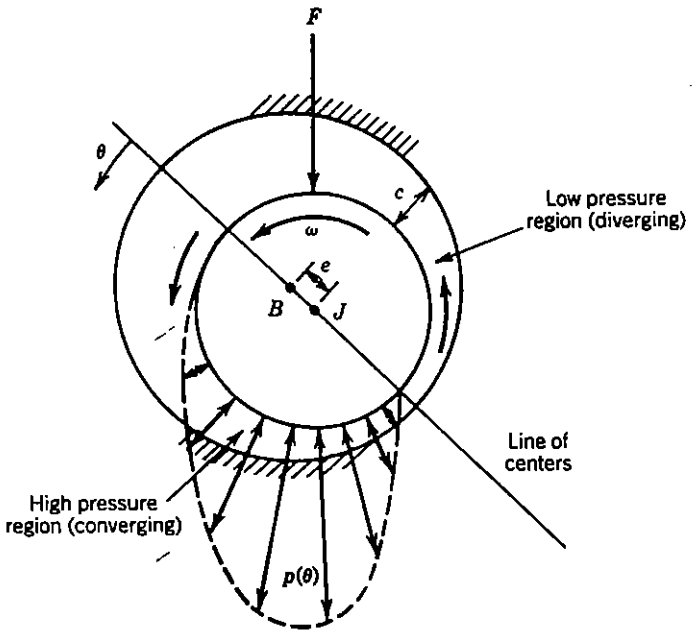

In tilting pad bearings, the pads are free to rotate about a pivot. Each pad adjusts such that the hydrodynamic reaction load passes through the pivot point. This adjustment of the pads eliminates creating cross-coupled forces, thus virtually eliminating the potential of whirl instability (oil whirl and oil whip).

Tilting Pad Bearing Geometry:

A schematic view of a tilting pad bearing geometry is given in Figure 5, and shows all the possible degrees of freedom in a tilting pad.

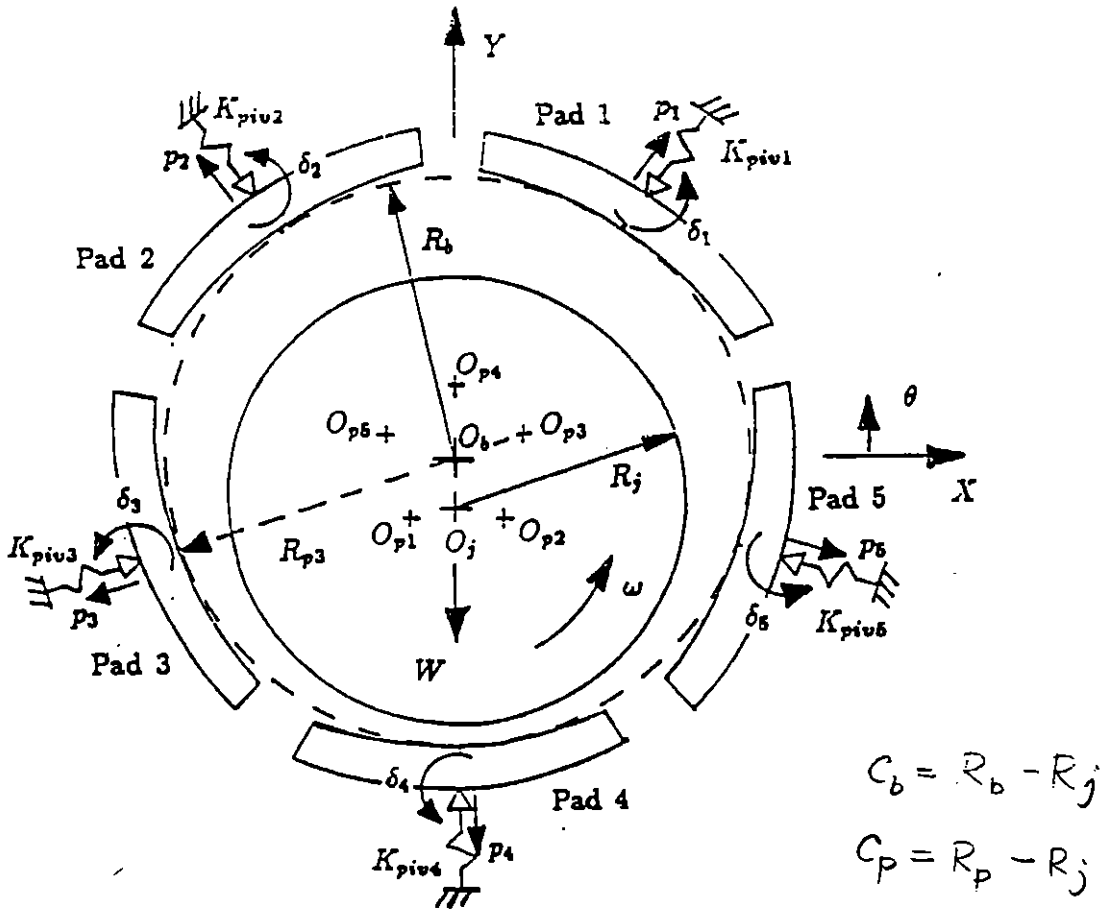

Figure 5. Schematic of 5-Shoe Load-On Pad Tilting Pad Journal Bearing

The **fluid film thickness** (h) in a pad is written as:

$$h = Cp_{ipad} + e_X \cos\theta + e_Y \sin\theta + (Cp_{ipad} - C_{Bipad}) \cos(\theta - \theta p_{ipad}) - \delta_{ipad} Rj \sin(\theta - \theta p_{ipad}).$$

Where (e_X , e_Y) are the journal center displacements, Cp_{ipad} and C_{bipad} are the pad and bearing clearances, and δ_{ipad} is the pad rotation.

The parameters controlling the static and dynamic characteristics of tilting pad bearings are:

(1) **Pivot Offset**: $\alpha = \theta p/\beta$

where β is the pad extent angle, and θp is the pivot angle measured from the pad leading edge. When $\alpha = 0.5$, the pads are centrally pivoted. The bearing load carrying capacity increases when the offset (α) increases. The optimum offset is $\alpha \approx 0.58$. Central pivoted bearings are widely used. Offset pivot bearings with $\alpha > 0.5$ are used in rotating machinery which will not run in reverse. The offset pivot ensures a converging wedge for all conditions.

(2) **Bearing Preload:** $m = \dfrac{C_p - C_b}{C_p}$

where $C_p = (R_p - R_j)$ is the pad clearance, and $C_b = (R_b - R_j)$, is the bearing clearance. The preload can vary from 0 to 1.0, with each pad having different radii, and hence different preload. When $R_p = R_b$ the preload is null, i.e. zero. Lightly loaded bearings are purposely preloaded to stiffen the rotor-bearing system. A typical preload is *m=0.3*. Negative preload are not unusual due to machining inaccuracies (stack up of tolerances) or errors on assembly and installation.

(3) **External loading condition**: The direction of loading also effects the static and dynamic force characteristics of a tilting pad bearing. The load can either be directed towards (on) a pad (*LOP*), or directed between the pads (*LBP*). The *LOP* configuration is chosen for lightly loaded bearings operating at high speed cases, whereas the *LBP* configuration is chosen for heavily loaded bearings. The *LOP* option renders different stiffness in the *X* and *Y* directions. Asymmetric stiffness is well known to increase rotor-bearing system stability

Analysis of tilting pad journal bearings:

A comprehensive tilting pad bearing analysis should include pad thermal and elastic effects along with the hydrodynamics of the fluid film. The thermal analysis encompasses shaft expansion effects, sump heating effects, pad thermal deformation effects, and hot oil carryover effects from pad to pad. Pivot deformation and pad elastic deformation due to pressure generation should also be considered. All these parameters have significant effects on the bearing load capacity and dynamic force coefficients. Figure 6 depicts a flow chart for the analysis.

Generalized Reynolds Equation:

The generalized Reynolds equation includes a variable fluid viscosity in the circumferential, axial, , and cross film directions, and given as

$$-\underline{\nabla}\cdot(C_1\underline{\nabla}P)+(\underline{\nabla}C_2)\cdot U+\frac{\partial h}{\partial t}=0$$

where $U=\Omega R/2$, C_1 and C_2 are integration coefficients of the fluid viscosity and

$$C_1=\int_0^h\int_0^z\frac{\xi}{\mu}d\,\xi\,dz-\frac{\int_0^h\frac{\xi}{\mu}d\xi}{\int_0^h\frac{1}{\mu}d\xi}\int_0^h\int_0^z\frac{1}{\mu}d\xi dz$$

defined as:

$$C_2=\frac{\int_0^h\int_0^z\frac{1}{\mu}d\xi dz}{\int_0^h\frac{1}{\mu}d\xi}$$

For a uniform (constant) lubricant viscosity across the film thickness, the Reynolds equation above takes the well known form:

$$-\underline{\nabla}\cdot\left(\frac{\rho h^3}{12\mu}\underline{\nabla}p\right)+\underline{\nabla}(\rho h)\cdot U+\frac{\partial(\rho h)}{\partial t}=0$$

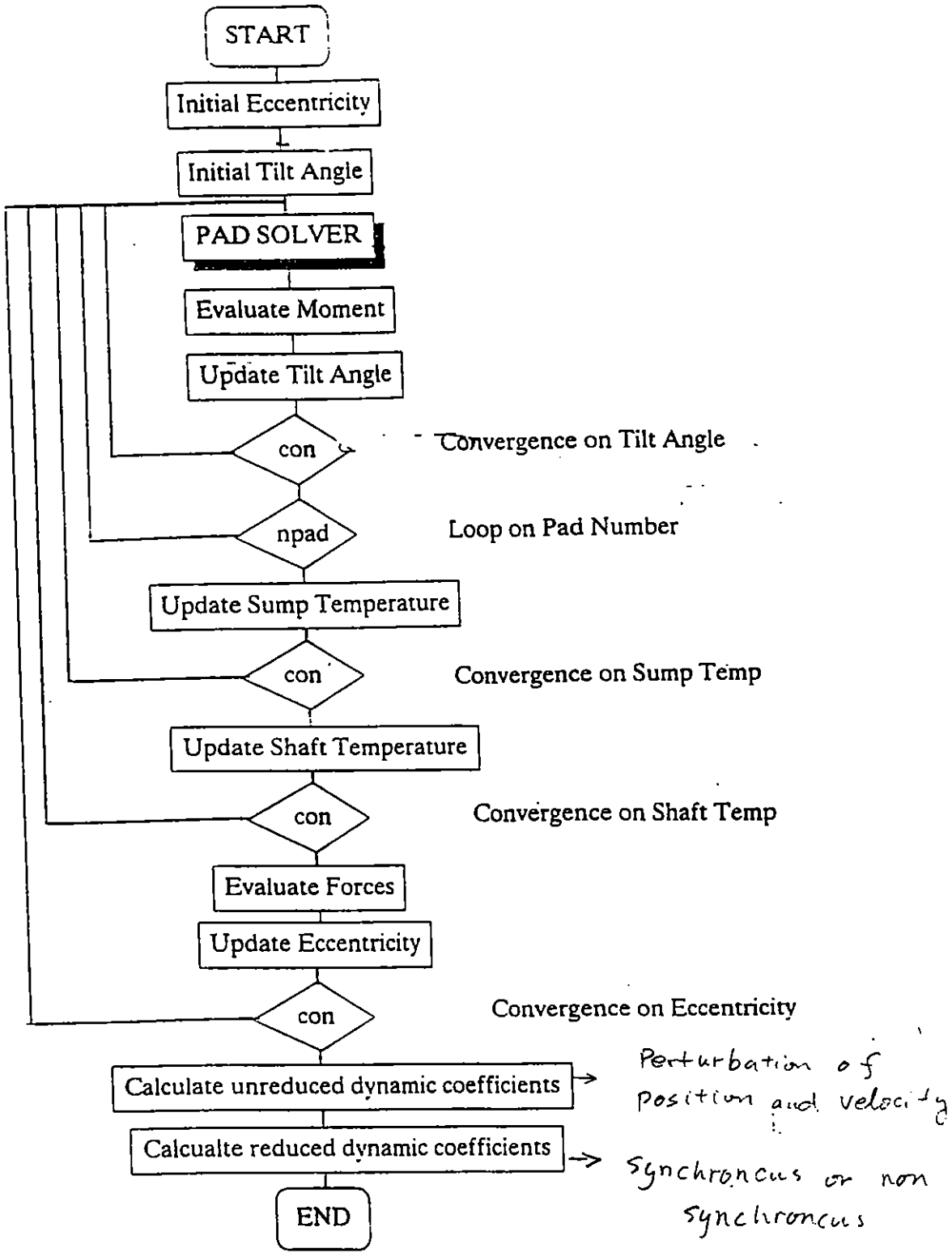

Figure 6. The flow diagram of global pad method

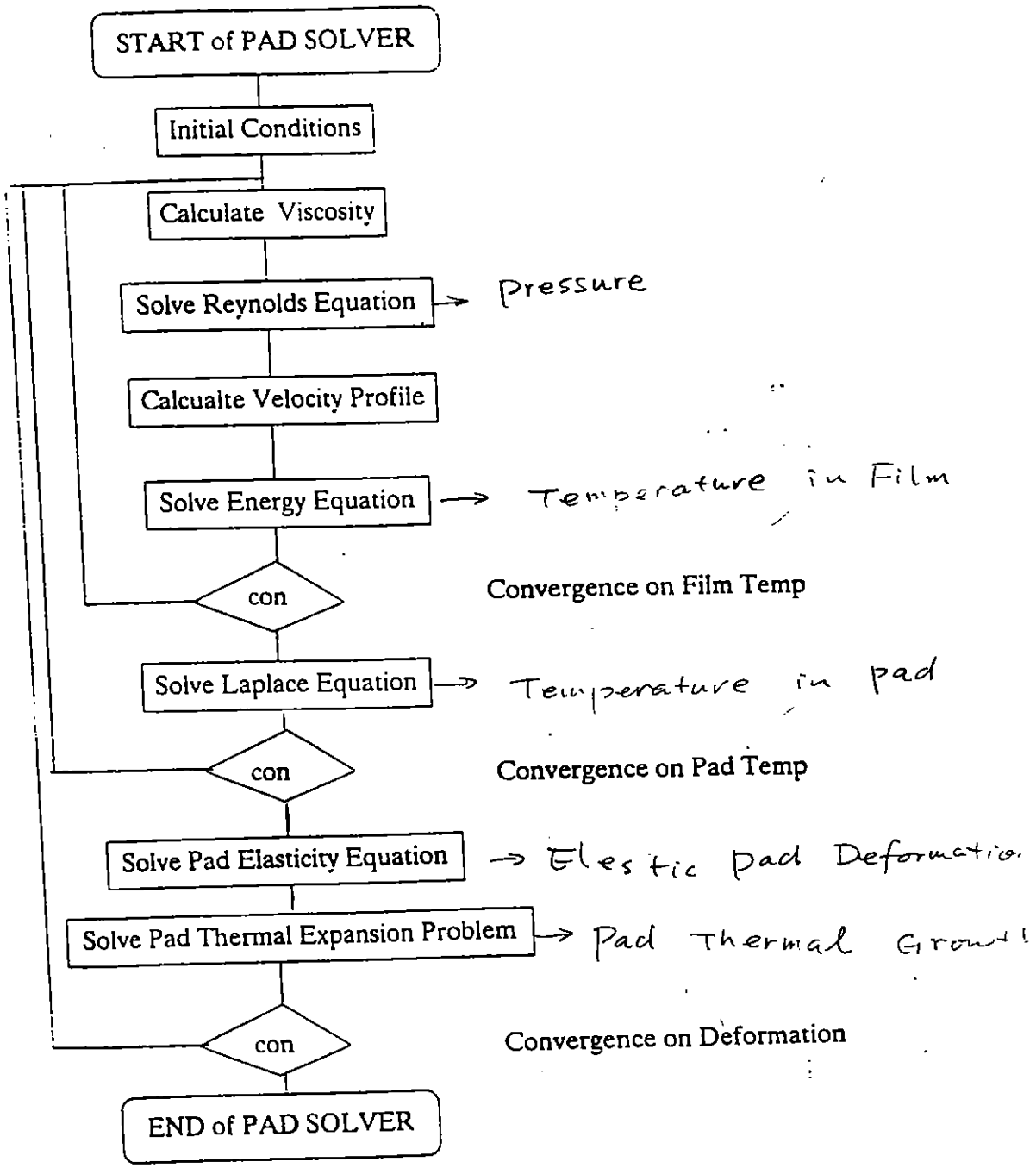

Figure 6 (Contd.) The flow diagram of the Pad Solver section

The assumptions used in deriving the generalized Reynolds equation are the same as given earlier in the class, except that the viscosity is regarded as non-uniform across the film thickness since significant temperature variations occur in the film thickness.

Boundary Conditions:

Only half a bearing pad needs to be analyzed due to symmetry if no journal misalignment is considered. The supply pressure is prescribed at the pad leading edge, and the discharge or exit pressure is given at the pad trailing edge and the pad outer boundary (z=L/2). A no axial flow condition is set at the pad center line.

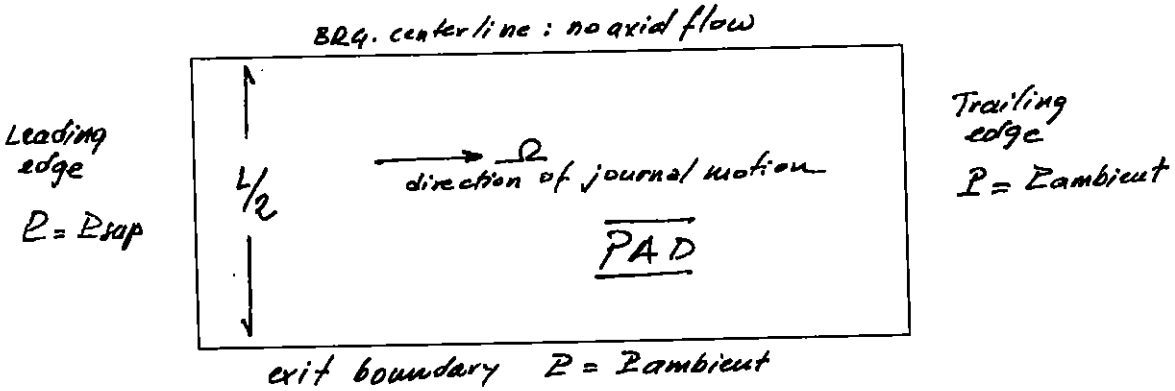

Lubricant cavitation occurs in the regions where the film thickness diverges. The most common approaches are:

(a) *Gumbel condition*: After solution of the Reynolds equation, all calculated pressures below the lubricant cavitation value are set to the cavitation value (and not included in the integration to obtain forces).

$$P = P_{CAV,} \quad if \quad P<P_{CAV}$$

Gumbel condition does not satisfy flow continuity within the cavitation zone.

(b) *Reynolds condition*: insures flow continuity at the position of film rupture, where the pressure is regarded as uniform and its normal gradient set to zero.

$$P = P_{cav} \quad and \quad \frac{\partial P}{\partial n} = 0 \quad if \quad P < P_{cav}$$

Figure 7 shows the pressure profiles obtained with these two boundary conditions. Note here that the *Sommerfeld* model does not disregard the pressures below the cavitation value.

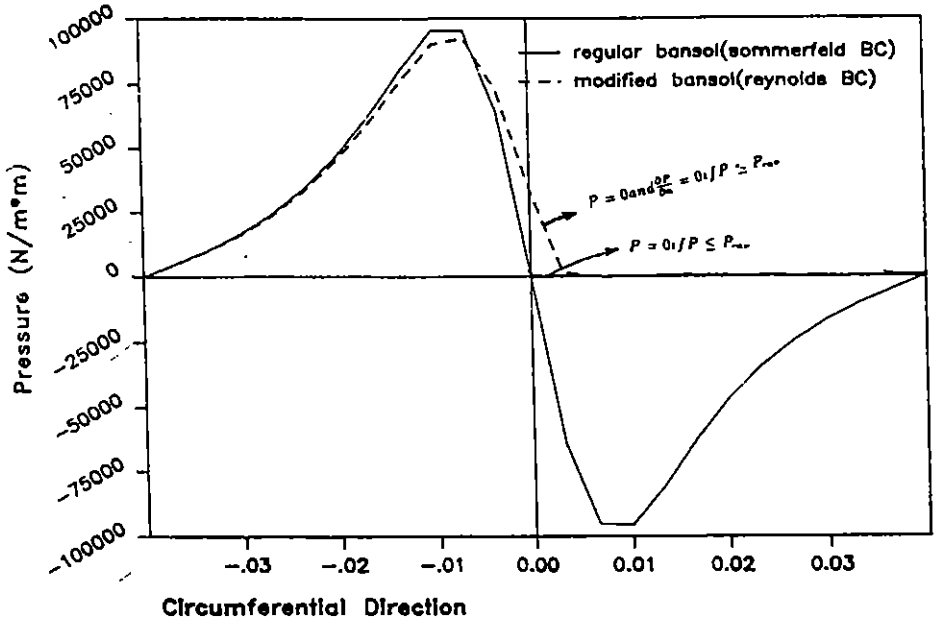

Figure 7.

Energy Transport Equation in the Fluid Film

The temperature distribution in the fluid film is coupled to the pressure distribution via the fluid viscosity. In isothermal cases, the fluid viscosity is not a function of temperature, and thus held constant. However, actual lubricant viscosity changes with temperature and pressure. The viscosity of typical mineral oils is a strong function of temperature, though its dependency on pressure is negligible for low pressures. There are several viscosity-temperature relationships, with the following one recommended for moderate temperature variations,

$$\mu = \mu_0 e^{-\beta(T-T_c)}; \quad \mu_0 = viscosity\ at\ T_0$$

$$\beta = temperature - viscosity\ coefficient\left(1/_{\circ F}\right)$$

According to the above equation, the viscosity changes as temperature changes. A change in viscosity will in turn affect the pressure distribution. A change in pressure distribution affects the velocity profiles, and these velocity profiles are used in the energy equation to predict the temperature field. This is how the Reynolds equation and energy equation are coupled.

The fluid film energy transport equation includes energy convection, heat conduction and dissipation of the mechanical energy, and is given (w/o pressure-volume work changes) as:

$$\rho c_P \underline{u} \cdot \underline{\nabla} T = \underline{\nabla} \cdot (k \underline{\nabla} T) + \Phi$$

where $$\Phi = \mu \left[\left(\frac{\partial u}{\partial x} \right)^2 + \left(\frac{\partial w}{\partial z} \right)^2 \right]$$

and, ρ is the fluid density [kg/m^3], C_P is the fluid specific heat [J/kg°C], $\underline{u}$ denote the fluid velocity vector [m/s], k is the fluid thermal conductivity [J.m/°C].

Studies and experiments have shown that the axial temperature variation is negligible, so the cross-film temperature distribution needs to be evaluated only the bearing centerline.

There is one problem with the numerical solution of the fluid energy transport equation. Whenever the convection term becomes significant, ($\rho C_p \underline{u} \cdot \underline{\nabla} T$), numerical oscillations occur in the solution, producing convergence problems. One way to avoid this problem is by using an upwinding scheme or by using a fine grid (satisfying the condition of small *Peclet* numbers).

Thermal Boundary Conditions:

At the **pad leading edge** the inlet temperature is either equal to the fluid supply temperature, T_{supply} , or a more common T_{mixing}, due to the mixing of the hot lubricant from the upstream pad with the cold lubricant from the feed. The mixing temperature is obtained from a simple thermal energy balance,

$$T_{mixing} = \frac{Q_{recir} T_{recir} + Q_{supply} T_{supply}}{Q_{recir} + Q_{supply}}.$$

where (Q_{recirc}, T_{recirc}) are the hot-carryover flow and temperature leaving the upstream pad. Figure 8 shows a schematic representation of the lubricant mixing

Fig 8.

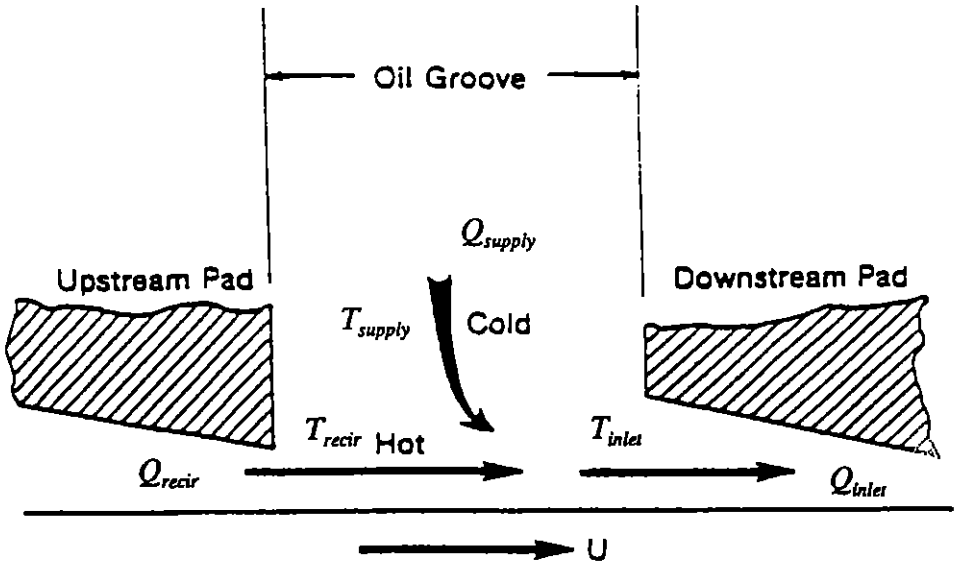

Shaft-Film Boundary: The shaft temperature is generally regarded as constant in the circumferential direction. There are three ways of finding the shaft temperature:

1) Constant shaft temperature obtained from experiments.

2) Shaft temperature equal to the average of the film temperatures (and updated in each calculation),

$$T_{SH} = \frac{1}{2\pi} \int_0^{2\pi} \left(\frac{1}{h} \int_0^h T dy \right) d\theta$$

(3) No heat flux around the shaft, i.e.

$$\int_0^{2\pi} k_{SH} \frac{\partial T_{SH}}{\partial n} d\theta = 0$$

This condition is checked after each shaft temperature calculation.

Continuity of temperatures and heat fluxes must be satisfied at the **film-pad interface.** At **the pad trailing edge and side edges,** no thermal boundary conditions are specified since the fluid flow typically leaves through these boundaries.

Cavitation: The lubricant film generally adheres to the rotating shaft as streamers when fluid cavitation occurs (see Figure 9). The fluid region adjacent to the pad is a gas, while the region next to the shaft is a liquid. Note that the pad is stationary and the whole liquid film adhering to the shaft moves at the shaft speed. Thus any viscous heating in the cavitation region is that of the vapor, and henceforth, very small. Measurements have shown that the fluid temperature actually drops in the cavitation zone, thus indicating that some heat is needed to vaporize the fluid.

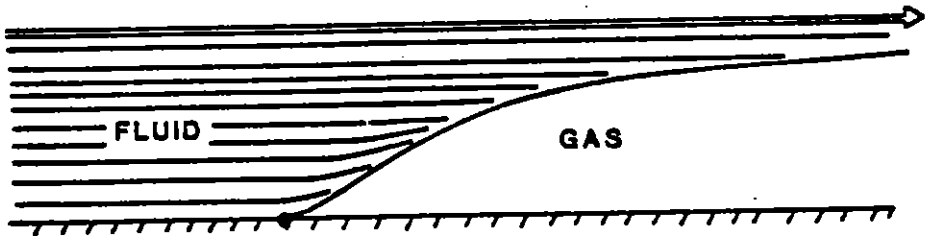

SIDE VIEW

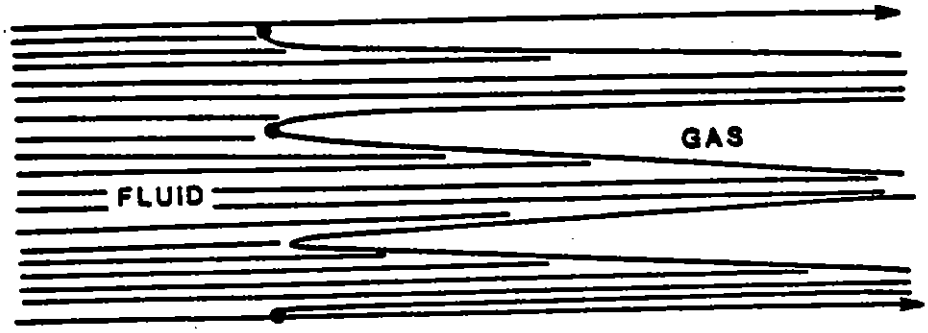

TOP VIEW

Heat Conduction In Pads:

The temperature distribution in the pads needs to be calculated as the pads expand when the temperature increases. The governing *Laplace* equation is

$$\underline{\nabla} \cdot \underline{\nabla} T = 0$$

and with the following boundary conditions:

(i) Pad - Fluid Film Interface: continuity of temperatures and heat fluxes

(ii) Sump temperature prescribed on all other pad boundaries.

Elastic And Thermal Deformation of Pads: The deformation of elastic structures is described by means of the constitutive relationship and equilibrium equation. The constitutive equation for an linearly elastic material is given as:

$$\underline{\underline{\sigma}} = \underline{\underline{C}}\,\underline{\underline{\varepsilon}} + \underline{\underline{\sigma}}_0$$

where $\underline{\underline{\sigma}}$ is the stress tensor, $\underline{\underline{\varepsilon}}$ is the strain tensor, and $\underline{\underline{\sigma}}_0$ is the residual stress tensor (typically due to thermal effects).

The equilibrium equations for a stationary elastic media are given by the following:

$$\underline{\nabla} \cdot \underline{\underline{\sigma}} + \underline{b} = \underline{f}$$

where $\underline{b}$ is the body force vector, and $\underline{f}$ is the load vector.

The pad deformation is composed as the linear superposition of elastic deflections due to the hydrodynamic pressure and thermal expansions due to the temperature gradients. Of course, the preceding assumes the deformations are small enough to warrant linearity. The temperature distribution from solution to the pad heat conduction equation is applied to obtain thermal expansion, while the fluid pressure is integrated to obtain forces. These forces are resolved into components in the X and Y directions and applied on the pad surface to obtain mean deformations.

Pivot Flexibility: The contact between a bearing pad and the supporting pivot occurs (typically) through a small contact area which can be easily susceptible to wear. Most tilting pad **pivots** show non-linear stiffnesses with a strong dependency on the applied load and must be evaluated by Hertzian contact models. Here, for simplicity we calculate the pivot deflection as in a simple spring model, i.e.

$$d_{piv} = \frac{F_{piv}}{K_{piv}}.$$

where K_{piv} is the pivot stiffness and F_{piv} is the component of the applied load passing through the pivot.

Thermal Expansion of the Shaft: is given as

$$\Delta D_{sh} = D_{sh}\, \alpha_{sh} \left(T_{sh} - T_{ref}\right).$$

where D_{sh} is the diameter of shaft and α_{sh} is the coefficient of thermal expansion for the shaft material. It can easily be seen that the fluid film thickness decreases as shaft thermal expansion increases.

Journal Static Equilibrium:

The most important aspect of the static equilibrium calculation is to find the pad equilibrium tilt angle. Figure 10 shows how the fluid film induced moment on a pad varies with pad tilt angle. Pad equilibrium is achieved when the fluid film moment on the pad equals zero. The forces on the pad are given by

$$\begin{Bmatrix} F_r \\ F_t \end{Bmatrix} = 2 \int_{\theta_L}^{\theta_T} \int_0^{L/2} p(\theta, z)\, \underline{n}(\theta)\, dz\, d\theta.$$

where $\underline{n} = cos\theta\ \underline{u}_r + sin\theta\ \underline{u}_t$ in the radial and tangential directions. The fluid moment on the pad is given by:

$$M = \int_{\theta_L}^{\theta_T} \int_O^{L/2} p(\theta, z)\, \underline{d} \times \underline{n}\, dz d\theta \text{ with } \underline{d} \text{ as a distance vector}$$

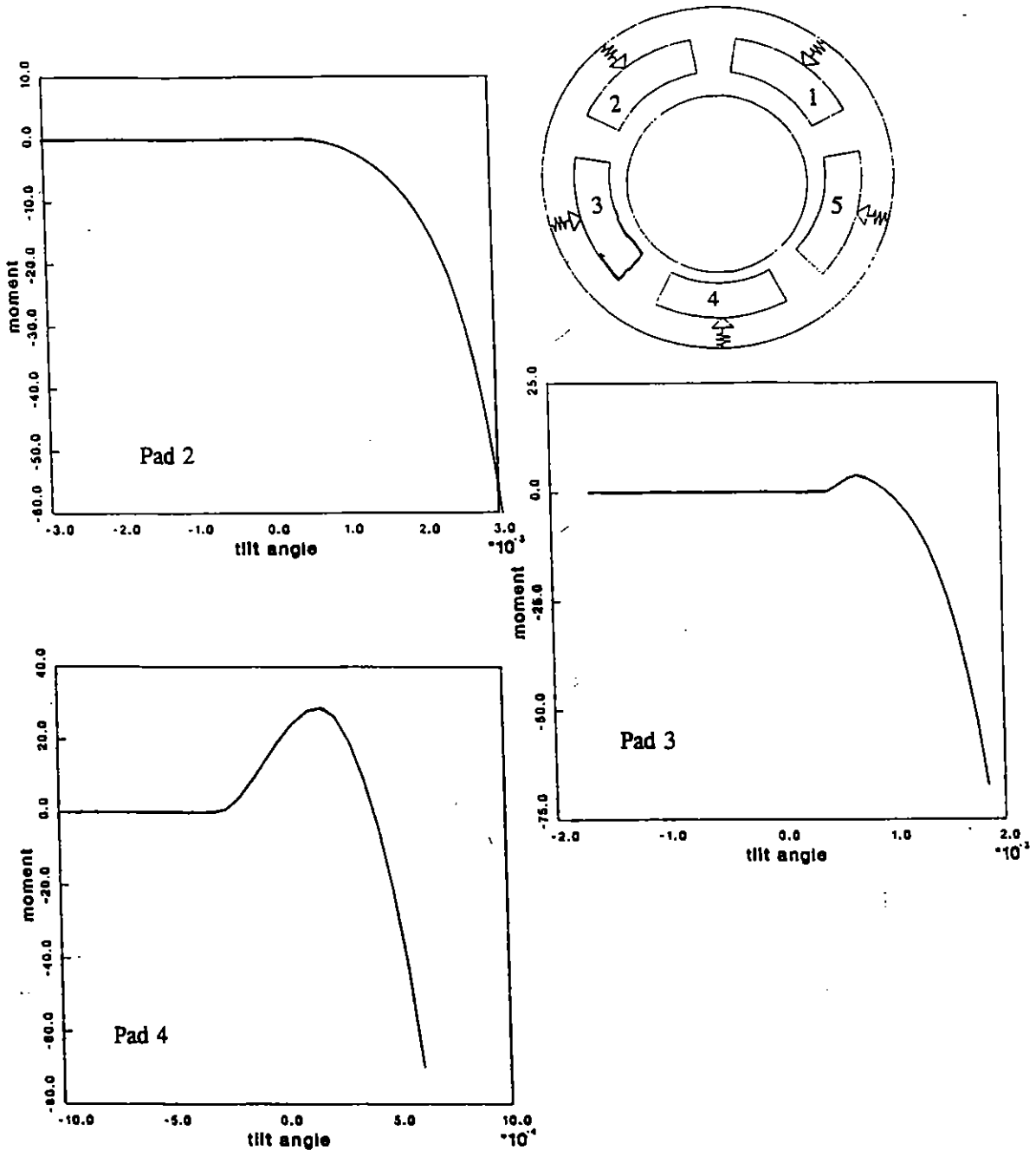

Figure 10. Graphs of moment versus pad tilt angles of a five shoe tilting pad journal bearing

Dynamic force coefficients of a tilting pad bearing:

Tilting pad bearing stiffness and damping force coefficients are obtained after the bearing static equilibrium is achieved. The pivot and pad tilt degrees of freedom should be included in determining the dynamic force coefficients. The stiffness coefficients are given by perturbing the journal position (X and Y), pad tilt angles (δ_{IPAD}), and pivot deformation (P_{IPAD}). The change in force/moments are obtained for these perturbations. The pad elastic deformation is represented as a change in the pad radius (R_{IPAD}). The relationship for the stiffness coefficients is

$$\begin{Bmatrix} \Delta F_x \\ \Delta F_Y \\ \Delta M_\delta \\ \Delta F_P \\ \Delta F_R \end{Bmatrix} = \begin{bmatrix} -K_{xx} & -K_{XY} & -K_{X\delta_{IPAD}} & -K_{XP_{IPAD}} & -K_{XR_{IPAD}} \\ -K_{yx} & -K_{YY} & -K_{Y\delta_{IPAD}} & -K_{YP_{IPAD}} & -K_{YR_{IPAD}} \\ -K_{\delta_{IPAD}x} & -K_{\delta_{IPAD}y} & -K_{\delta\delta} & -K_{\delta P_{IPAD}} & -K_{\delta R_{IPAD}} \\ -K_{P_{IPAD}x} & -K_{P_{IPAD}y} & -K_{P_{IAD}\delta} & -K_{PP_{IPAD}} & -K_{PR_{IPAD}} \\ -K_{R_{IPAD}X} & -K_{R_{IPAD}Y} & -K_{R_{IPAD}\delta} & -K_{R_{IPAD}P} & -K_{RR_{IPAD}} \end{bmatrix} \begin{Bmatrix} \Delta X \\ \Delta Y \\ \Delta\delta_{IPAD} \\ \Delta P_{IPAD} \\ \Delta R_{IPAP} \end{Bmatrix}$$

Each of these coefficients could be found by numerical perturbation of the form:

$$K_{XX} = -\frac{F_X(\Delta_X) - F_X(-\Delta_X)}{2\Delta_X}$$

$$K_{XY} = -\frac{F_X(\Delta_Y) - F_X(-\Delta_Y)}{2\Delta_Y}$$

$$K_{X\delta_{IPAD}} = -\frac{F_X(\Delta\delta) - F_X(-\Delta\delta)}{2\Delta\delta}$$

$$K_{XP_{IPAD}} = -\frac{F_X(\Delta P) - F_X(-\Delta P)}{2\Delta P}$$

$$K_{XR_{IPAD}} = -\frac{F_X(\Delta R) - F_X(-\Delta R)}{2\Delta R}$$

'IPAD' as a subscript indicates I^{th} pad.

In current computational procedures. The fluid flow equations are perturbed for small amplitude motions for each degree of freedom, and the force coefficients obtained from first-order pressure fields.

The total number of degrees of freedom per bearing is equal to

$(2 + 3\text{x}N_{pad})$ where N_{pad} is the number of pads

Damping coefficients are found in a similar manner, except that velocities are perturbed instead of displacements.

Coefficient Reduction Most rotor-bearing stability programs can accept only 4 stiffness and 4 damping force coefficients. The extra degrees of freedom need to be removed to obtain the reduced force coefficients. Reduced coefficients can be synchronous or nonsynchronous, depending on the assumed pad frequency of motion. The general equations of motion for the unreduced force coefficients are:

$$\begin{bmatrix} \underline{\underline{M}}_{mm} & \underline{\underline{M}}_{ms} \\ \underline{\underline{M}}_{sm} & \underline{\underline{M}}_{ss} \end{bmatrix} \begin{Bmatrix} \ddot{\underline{X}}_m \\ \ddot{\underline{X}}_s \end{Bmatrix} + \begin{bmatrix} \underline{\underline{C}}_{mm} & \underline{\underline{C}}_{ms} \\ \underline{\underline{C}}_{sm} & \underline{\underline{C}}_{ss} \end{bmatrix} \begin{Bmatrix} \dot{\underline{X}}_m \\ \dot{\underline{X}}_s \end{Bmatrix}$$

$$+ \begin{bmatrix} \underline{\underline{K}}_{mm} & \underline{\underline{K}}_{ms} \\ \underline{\underline{K}}_{sm} & \underline{\underline{K}}_{ss} \end{bmatrix} \begin{Bmatrix} \underline{X}_m \\ \underline{X}_s \end{Bmatrix} = \begin{Bmatrix} \underline{F}_m \\ \underline{O} \end{Bmatrix}$$

where the subindices '=' and '-▭' indicate matrices and vectors, respectively. '*m*' indicates the *master* degrees of freedom (*X,Y* journal center motions), and '*s*' indicates the *slave* degrees of freedom, i.e. the pad degrees of freedom.

Assume a frequency (ν) for the journal center and pad motions, i.e.,

$$\begin{Bmatrix} \Delta x \\ \Delta y \\ \Delta \delta_{IPAD} \\ \Delta P_{IPAD} \\ \Delta F_X \\ \Delta F_Y \\ \Delta F_{R_{IPAD}} \end{Bmatrix} = e^{-i\nu t} \begin{Bmatrix} \Delta \hat{x} \\ \Delta \hat{y} \\ \Delta \hat{\delta}_{IPAD} \\ \Delta \hat{P}_{IPAD} \\ \Delta \hat{F}_X \\ \Delta \hat{F}_Y \\ \Delta \hat{R}_{IPAD} \end{Bmatrix}$$

Substituting these into the equations of motion leads to:

$$-\nu^2 \begin{bmatrix} \underline{\underline{M}}_{mm} & \underline{\underline{O}} \\ \underline{\underline{O}} & \underline{\underline{O}} \end{bmatrix} \begin{Bmatrix} \hat{\underline{X}}_m \\ \hat{\underline{X}}_s \end{Bmatrix} + i\nu \begin{bmatrix} \underline{\underline{C}}_{mm} & \underline{\underline{C}}_{ms} \\ \underline{\underline{C}}_{sm} & \underline{\underline{C}}_{ss} \end{bmatrix} \begin{Bmatrix} \hat{\underline{X}}_m \\ \hat{\underline{X}}_s \end{Bmatrix} + \begin{bmatrix} \underline{\underline{K}}_{mm} & \underline{\underline{K}}_{ms} \\ \underline{\underline{K}}_{sm} & \underline{\underline{K}}_{ss} - \nu^2 \underline{\underline{M}}_{ss} \end{bmatrix} \begin{Bmatrix} \hat{\underline{X}}_m \\ \hat{\underline{X}}_s \end{Bmatrix} = \begin{Bmatrix} \hat{\underline{F}}_m \\ \underline{O} \end{Bmatrix}$$

Rearranging the above equation and using complex matrix algebra,

$$\begin{bmatrix} \underline{\underline{Z}}_{mm} & \underline{\underline{Z}}_{ms} \\ \underline{\underline{Z}}_{sm} & \underline{\underline{Z}}_{ss} \end{bmatrix} \begin{Bmatrix} \underline{\hat{X}}_m \\ \underline{\hat{X}}_s \end{Bmatrix} = \nu^2 \begin{bmatrix} \underline{\underline{M}}_{mm} & \underline{\underline{O}} \\ \underline{\underline{O}} & \underline{\underline{O}} \end{bmatrix} \begin{Bmatrix} \underline{\hat{X}}_m \\ \underline{\hat{X}}_s \end{Bmatrix} + \begin{Bmatrix} \underline{\hat{F}}_m \\ \underline{O} \end{Bmatrix}$$

After a *Guyan* reduction, i.e. elimination of the *slave DOF*,

$$\underline{\underline{Z'}}_{mm} \underline{\hat{X}}_m = \nu^2 \underline{\underline{M}}_{mm} + \underline{F}_m$$

and

$$\underline{\underline{Z'}}_{mm} = \underline{\underline{Z}}_{mm} - \underline{\underline{Z}}_{ms} \underline{\underline{Z}}_{ss}^{-1} \underline{\underline{Z}}_{sm}$$

The frequency reduced stiffness and damping force coefficients are

$$\begin{bmatrix} K^*_{XX} & K^*_{XY} \\ K^*_{YX} & K^*_{YY} \end{bmatrix} = Real(\underline{\underline{Z}}'_{mm})$$

$$\begin{bmatrix} C^*_{XX} & C^*_{XY} \\ C^*_{YX} & C^*_{YY} \end{bmatrix} = \frac{1}{\nu} Imag(\underline{\underline{Z}}'_{mm})$$

Results:

Pre-load effects:

Figure 11 shows that the stiffness and damping force coefficients increase with an increase in pad preload.

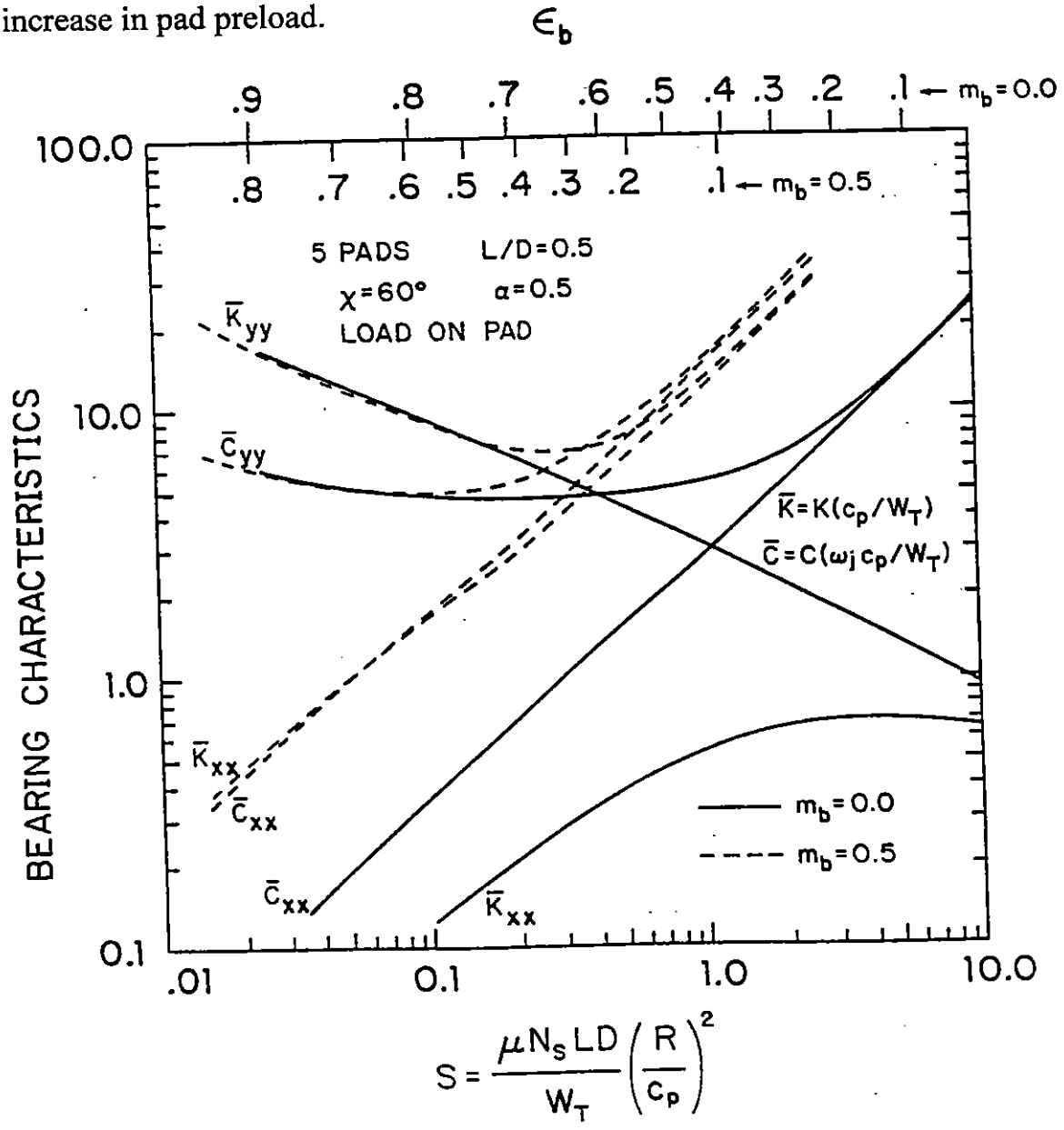

Figure 11. Tilting Pad Bearing Characteristics - The Effect of Changing The Bearing Preload from $m_b = 0.0$ to $m_b = 0.5$ for the Load on Pad condition. Centrally Pivoted Bearing.

Effect of load direction:

For the load on pad *(LOP)*, the stiffness and damping coefficients are significantly different in the X and Y directions. On the other hand, the force coefficients are very similar for the load between pad *(LBP)* as seen in Figure 12.

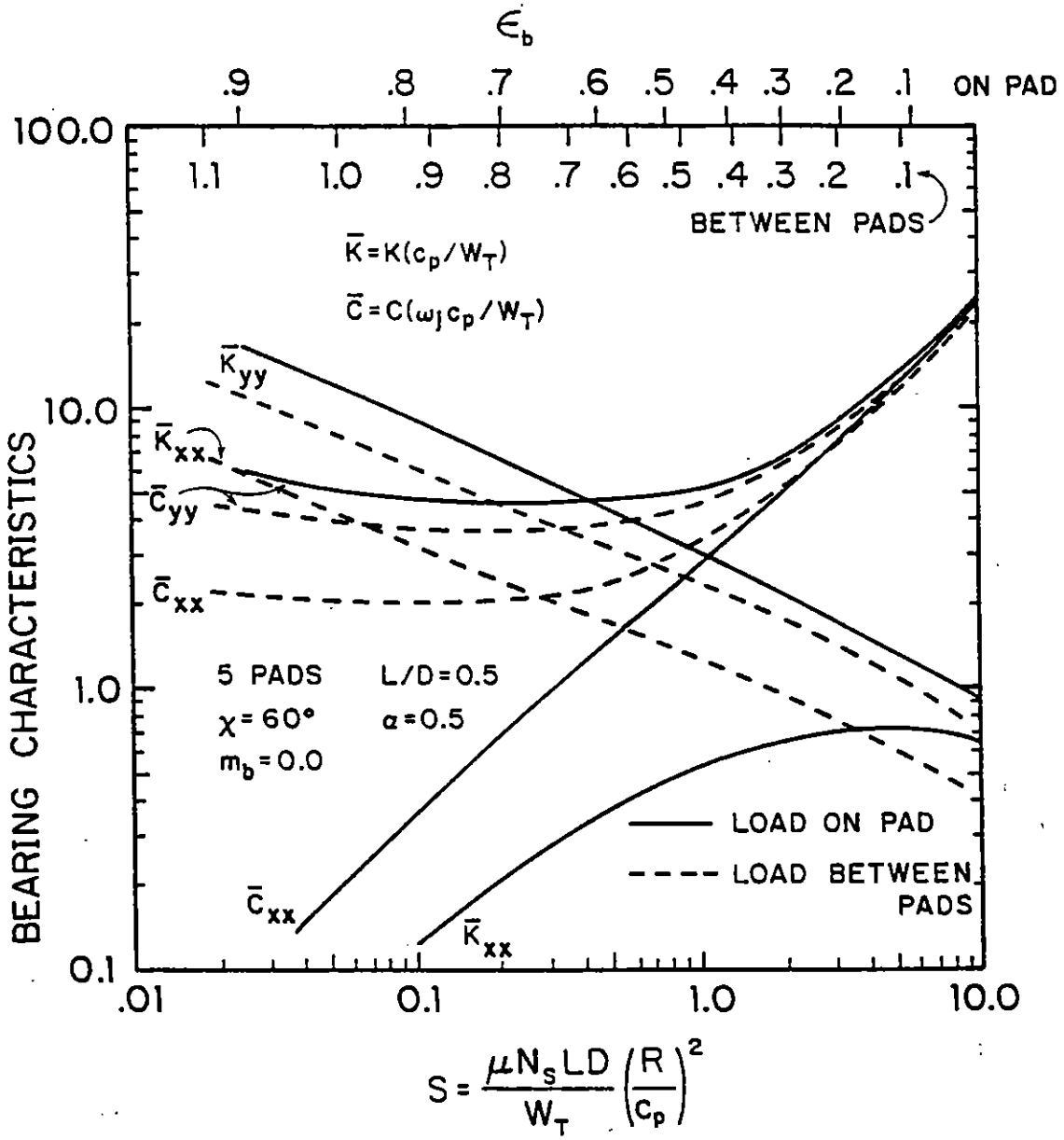

Figure 12. Tilting Pad Bearing Characteristics - The Effect of Changing Pad Loading from *Load on Pad* to *Load Between Pads* for the Zero Pre-load, Centrally Pivoted Bearing.

Pivot Offset Effects:

As the pad offset increases, the X-stiffness and damping coefficients increase significantly. However, not a large change is observed in the vertical direction coefficients.

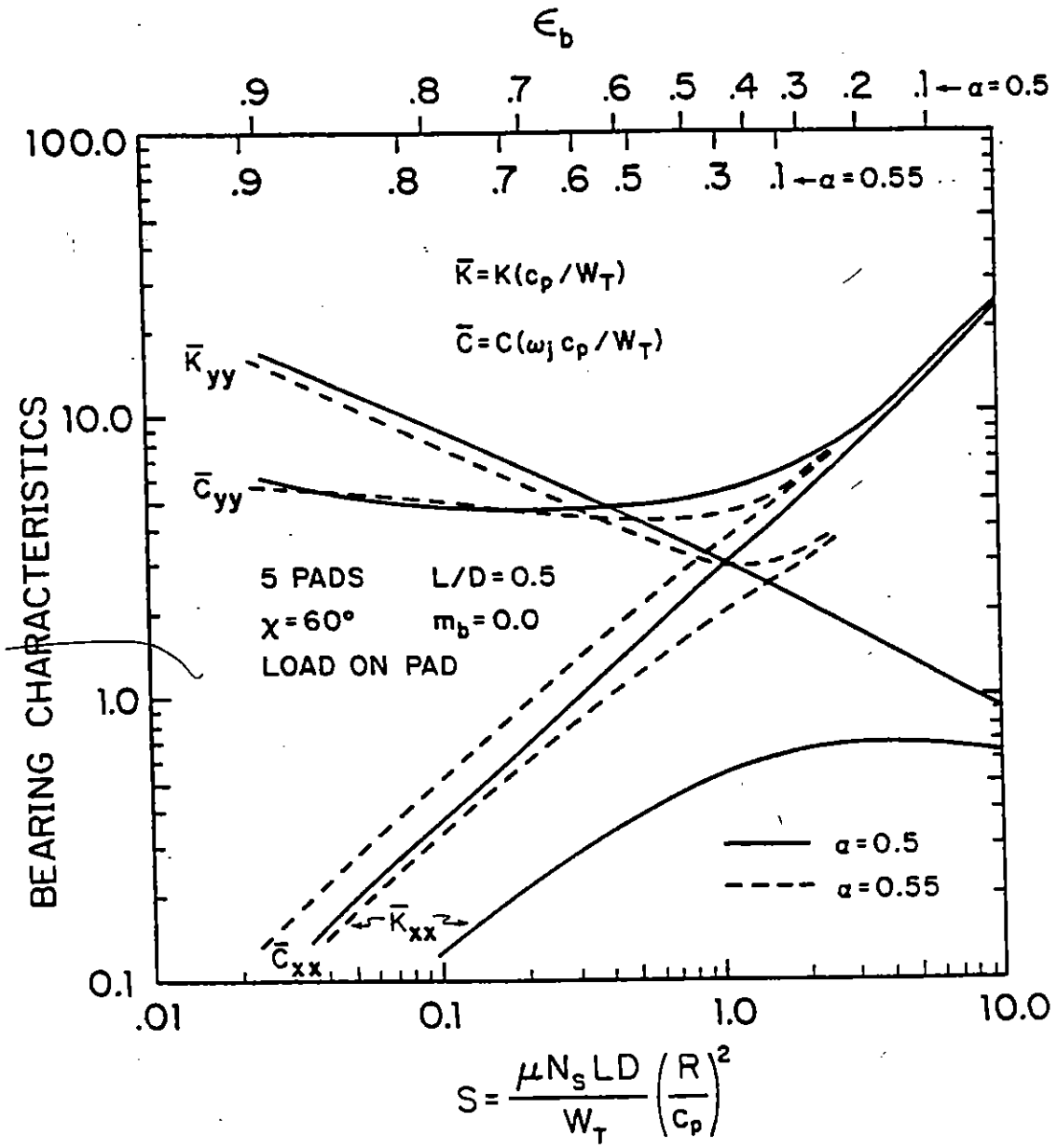

Figure 13. Tilting Pad Bearing Characteristics - The Effect of Changing Offset Factor from $\alpha = 0.5$ (Centrally Pivoted) to $\alpha = 0.55$ for the *Load on Pad*, Zero preload bearing.

Effects of Various Types of Analyses:

Figures 14 through 16 show the effect of using various types of analysis to predict the dynamic force coefficient and damping exponent of a simple rotor supported on tilting pad bearings. The acronyms are as follows, *HD* : Hydrodynamic, *THD* : thermohydrodynamic; *EHD* : Elastohydrodynamic; *TEHD* : Thermoelastohydrodynamic.

The *THD* analysis predicts the larget stiffness and damping force coefficients. Note that the stability of a system is reduced significantly when a complete *TEHD* analysis is performed.

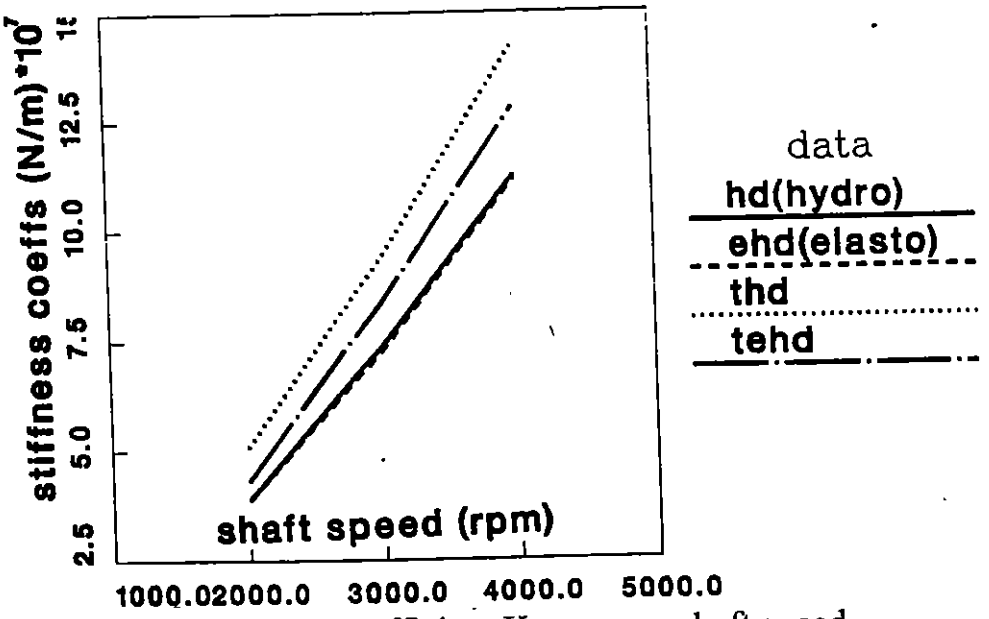

Figure 14. Stiffness coefficient K_{XX} versus shaft speed

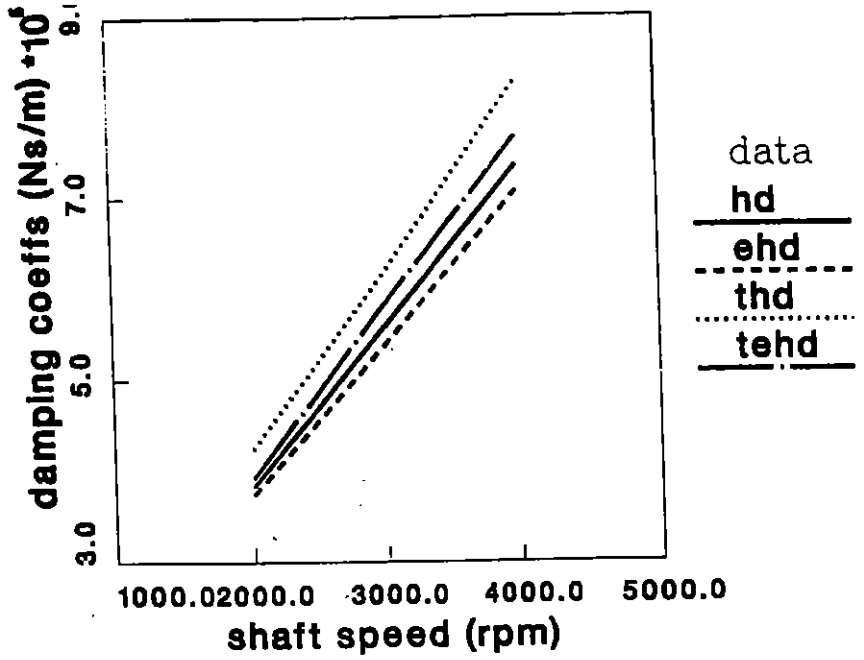

Figure 15. Damping coefficient C_{XX} versus shaft speed

Figure 16. Damping exponent versus shaft speed

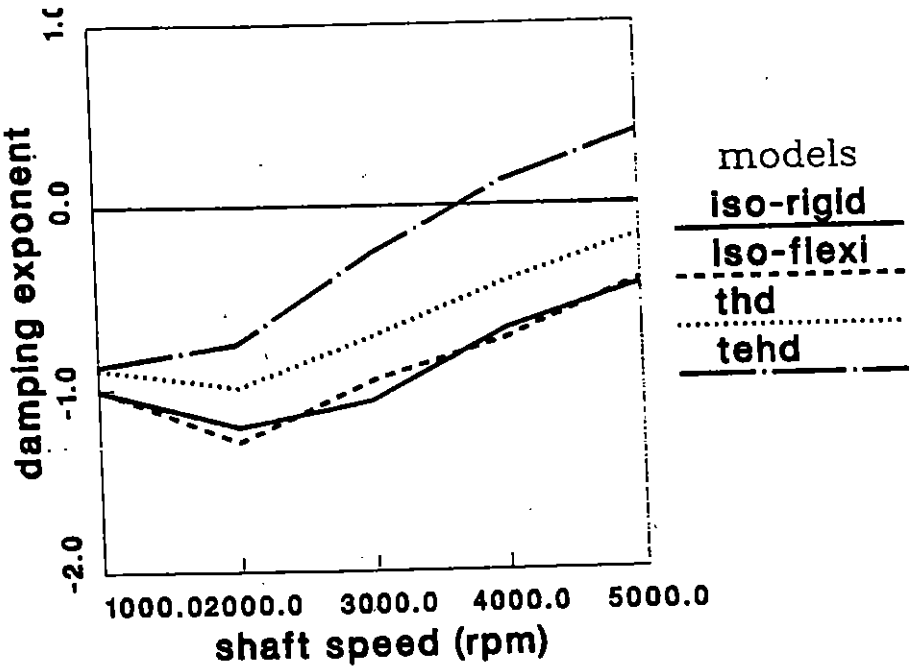

Pivot Stiffness Effects: Stiffness and damping force coefficients decrease as the pivot stiffness decreases.

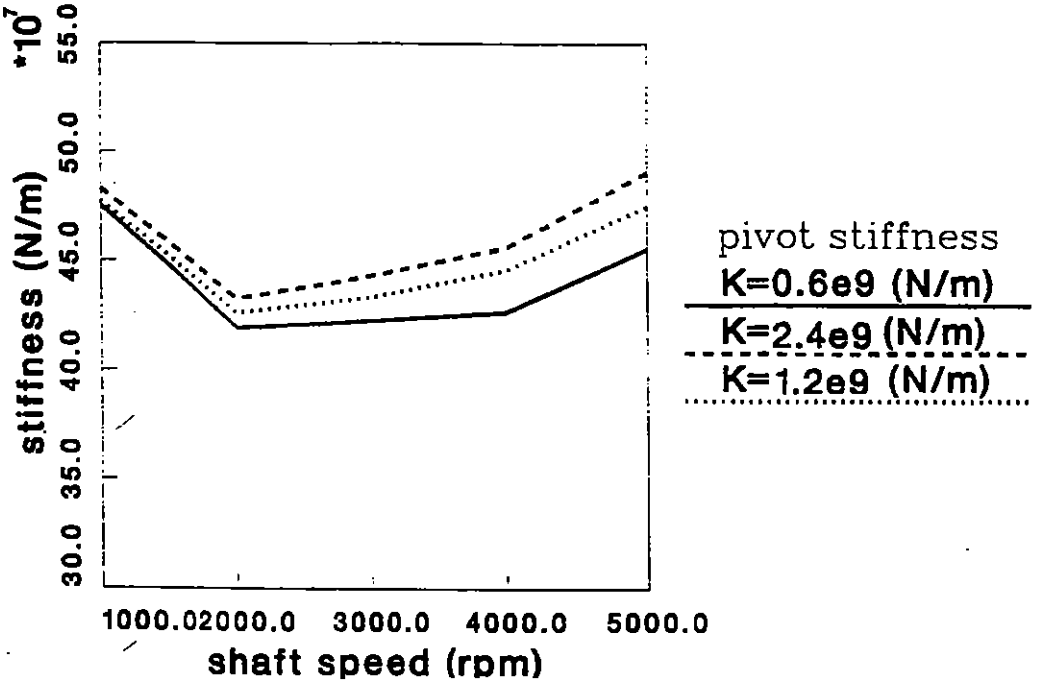

Figure 17. Stiffness coefficient versus shaft speed

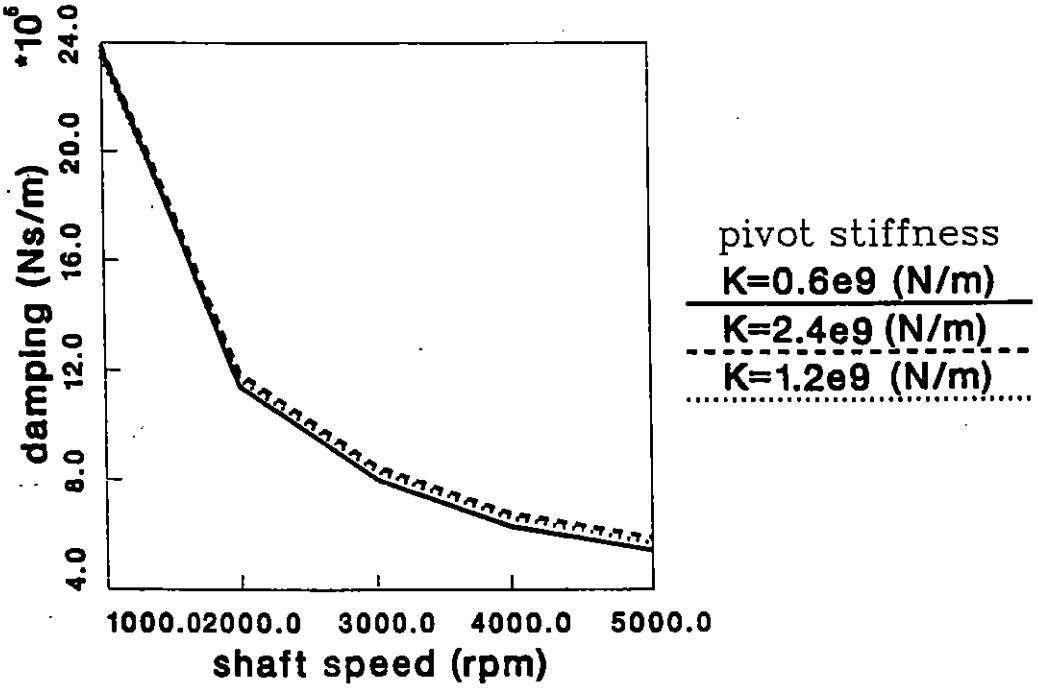

Figure 18. Damping coefficient versus shaft speed

Effect of Using Synchronously Reduced Coefficients:

Figure 19 shows a comparison of stability analysis with synchronously reduced force coefficients and unreduced force coefficients. Using synchronously reduced coefficients overpredicts the threshold speed of inestability. When eigenvalue dependent force coefficients are used, the instability speed is reduced by almost 2,000 rpm.

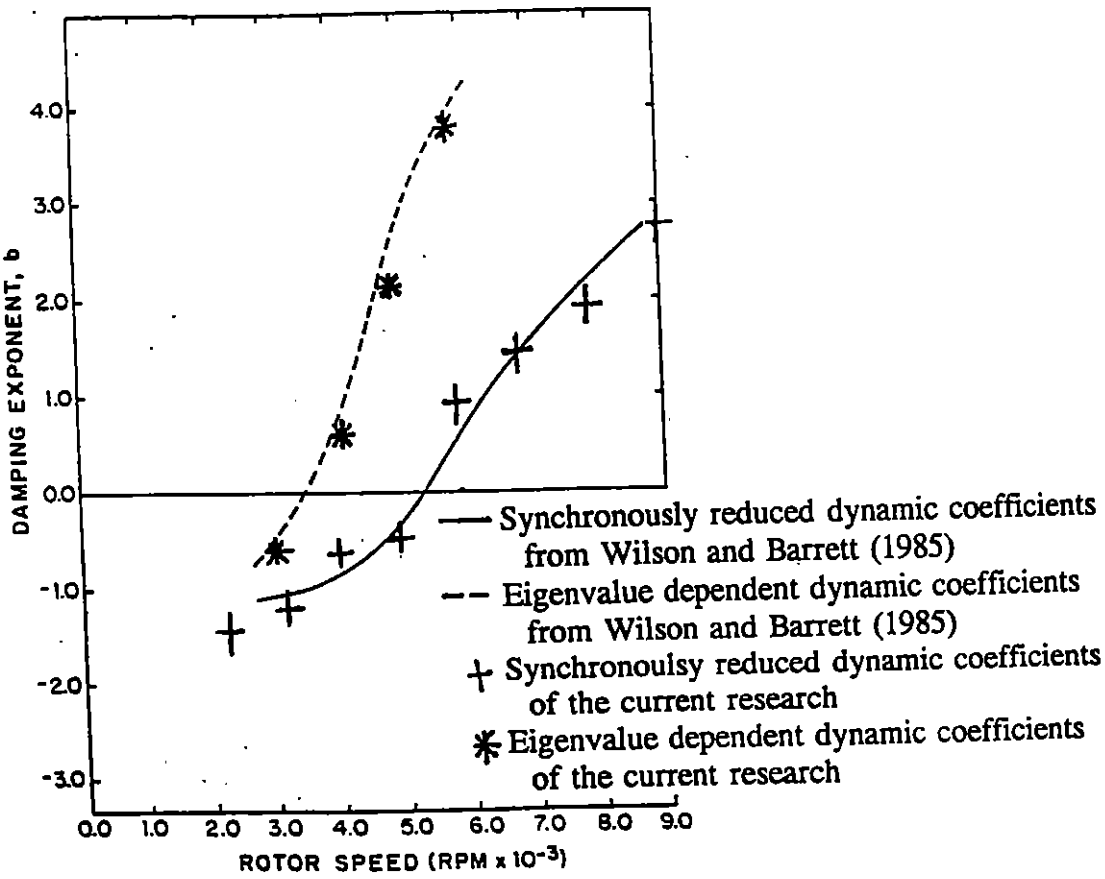

Figure 19.

TILTING PAD BEARINGS USEFUL REFERENCES:

Armentrout, R., and D. Paquette, 1993, "Rotordynamic Characteristics of Flexure-Pivot Tiliting Pad Journal Bearings," STLE Tribology Transactions, Vol 36, 3, pp. 443-451.

Arumugam, P., S. Swarnamani, and B.S. Prabhu, 1994, "Experimental Identification of Linearized Oil Film Coefficients of Cylindrical and Tilting Pad Bearings," ASME Paper 94-GT-81.

Barrett, L.E., Allaire P.E.,and B.W. Wilson, 1988, "The Eigenvalue Dependence of Reduced Tilting Pad Bearing Stiffness and Damping Coefficients," STLE Tribology Transactions, Vol. 31, 4, pp. 411-419.

Bouard, L., Fillon, M., and J. Frene, 1994, "Comparison Between Three Turbulent Models - Application to Themohydrodynamic Performances of Tilting-Pad Bearings," International Tribology Conference, AUSTRIB '94, Perth, Australia, December, pp. 119-126.

Brockwell,K., and D. Kleibub, 1989, "Measurement of the Steady State Operating Characteristics of the Five Shoe Tilting Pad Journal Bearing," STLE Tribology Transactions, Vol. 32, 2, pp. 267-275.

Brockwell,K., D. Kleibub, W. Dmochowski, 1990, "Measurement and Calculation of the Dynamic Operating Characteristics of the Five Shoe Tilting Pad Journal Bearing," STLE Tribology Transactions, Vol. 33, 4, pp. 481-492.

Chen, W.J., 1994, "Bearing Dynamic Coefficients of Flexible Pad Bearings," STLE Transactions, Preprint No. 94-TC-4D-1.

De Choudhury, P., M. Hill, and D. Paquette, "A Flexible Pad Bearing System for a High Speed Centrifugal Compressor," Proceedings of the 21st Turbomachinery Symposium, Dallas, TX, September, 1992, pp. 57-65.

Ettles, C., and A. Cameron, 1968, "Considerations of Flow Across a Bearing Groove, Journal of Lubrication Technology, pp. 312-319.

Ettles, C.M., 1980, "The Analysis and Performance of Pivoted Pad Journal Bearings Considering Thermal and Elastic Effects," ASME Journal of Lubrication Technology, Vol. 102, pp. 182-192.

Ettles, C.M., 1992, "The Analysis of Pivoted Pad Journal Bearing Assemblies Considering Thermoelastic Deformation and Heat Transfer Effects," STLE Tribology Transactions, Vol. 35, 1, pp. 156-162.

Fillon, M., J-C Bligoud, and J. Frene, 1991, "Experimental Study of Tilting-Pad Journal Bearings-Comparison with Theoretical Thermoelastohydrodynamic Results," ASME Transactions, Paper 91-trib-17.

Fillon, M., Frene, J., and R. Boncompain, 1987, "Historical Aspects and Present Development on Thermal Effects in Hydrodynamic Bearings," Proceedings of the 13th Leeds-Lyon Symposium, pp. 27-47.

Flack, R.D., and P.E. Allaire, 1984, "Literature Review of Tilting Pad and Turbulent Hydrostatic Journal Bearings for Nuclear Main Coolant Pumps," The Shock and Vibration Digest, Vol. 16, 7, pp. 3-12.

Flack, R.D., and C.J. Zuck, 1988, "Experiments on the Stability of Two Flexible Rotors in Tilting Pad Bearings," STLE Tribology Transactions, Vol. 31, 2, pp. 251-257.

Ha, H.C., Kim, H.J., and K.W. Kim, 1994, "Inlet Pressure Effects on the Thermohydrodynamic Performance of a Large Tilting Pad Journal Bearing," ASME Paper 94-Trib-26.

Kim, J., and A. Palazzolo, 1993, "Dynamic Characteristics of TEHD Tilt Pad Journal Bearing Simulation Including Multiple Mode Pad Flexibility Model," ASME 1993 Vibrations Conference, Vibrations of Rotating Systems, DE-Vol. 60,
pp. 363-379.

Knight, J.D., and L.E. Barrett, 1988, "Analysis of Tilting Pad Journal Bearings with Heat Transfer Effects," ASME Journal of Tribology, Vol. 110, pp. 128-133.

Lund, J., 1964, "Spring and Damping Coefficients for the Tilting Pad Journal Bearing," ASLE Transactions, Vol. 7, pp. 342-352.

Lund, J., and L. Bo Pedersen, 1986, "The Influence of Pad Flexibility on the Dynamic Coefficients of a Tilting Pad Journal Bearing," ASME Paper 86-Trib-49.

Mitsui, J.,Hori, Y., and M. Tanaka, 1983, "Thermohydrodynamic Analysis of Cooling Effect of Supply Oil in Circular Journal Bearing," ASME Journal of Lubication Technology, Vol. 105, pp. 414-421.

Nicholas, J.C., and R.G. Kirk, 1979, "Selection and Design of Tilting Pad and Fixed Lobe Journal Bearings for Optimum Rotordynamics," Proc. of the 8th Turbomachinery Symposium, Turbomachinery Laboratory, Texas A&M University, Dallas, pp. 43-58.

Nicholas, J.C., and L.E. Barrett, 1986, "The Effect of Bearing support Flexibility on Critical Speed Predcition," ASLE Transactions, Vol. 29, 3, pp. 329-338.

Nicholas, J.C., 1994, "Tilting Pad Design," Proc. of the 23th Turbomachinery Symposium, Turbomachinery Laboratory, Texas A&M University, Dallas, pp. 179-194.

Orcutt, F.K., 1967, "The Steady-State Characteristics of the Tilting-Pad Journal Bearing in Laminar and Turbulent Flow Regimes," ASME Journal of Lubrication Technology, pp. 392-404

Parkins, D. W., and D. Horner, 1992, "Tilting pad Journal Bearings - Measured and Predicted Stiffness Coefficients,"STLE Transactions, Pre-print No. 92-TC-3D-2.

Pinkus, O., 1984/85, "Optimization of Tilting Pad Journal Bearings Including Turbulence and Thermal Effects," Israel Journal of Technology, Vol. 22, pp. 142-154.

Rouch, K.E., 1983, "Dynamics of Pivoted-Pad Journal Bearings, Including Pad Transalation and Rotation Effects," ASLE Transaction, Vol. 26, 1, pp. 102-109.

San Andrés, L.A., 1996,"Turbulent Flow, Flexure-Pivot Hybrid Bearings for Cryogenic Applications," ASME *Journal of Tribology*, Vol. 118, 1, pp. 190-200, (ASME Paper 95-TRIB-14).

Someya, T., (editor), "Journal-Bearing Databook," Springer-Verlag, 1988.

Taniguchi, S., T. Makino, K. Takeshita, T. Ichimura, "A Thermohydrodynamic Analysis of Large Tilting-Pad Journal Bearing in Laminar and Turbulent Flow Regimes with Mixing," ASME Journal of Tribology, Vol. 112, pp. 542-549, 1990.

White, M.F., and S.H. Chan, 1992, "The Subsynchronous Behavior of Tilting-Pad Journal Bearings," ASME Journal of Tribology, Vol. 114, pp. 167-173.

Zeidan, F., 1992, "Developments in Fluid Film Bearing Technology," Turbomachinery International Magazine, September/October 1992.

Zeidan, F., and D. J. Paquette, 1994, "Application of High Speed and High Performance Fluid Film Bearings in Rotating Machinery," Proc. of the 23th Turbomachinery Symposium, Turbomachinery Laboratory, Texas A&M University, Dallas, pp. 209-234.